Pure appl. geophys. 160 (2003) 2189–2221
0033–4553/03/112189–33
DOI 10.1007/s00024-003-2426-9

Pure and Applied Geophysics

Normal Mode Energetics for Far-field Tsunamis Generated by Dislocations and Landslides

EMILE A. OKAL[1]

Abstract—We apply the normal mode representation of tsunami waves, as introduced by WARD (1980) to the systematic study of the excitation of far-field tsunamis by both dislocation sources (represented by double-couples of moment M_0), and landslides (represented by single forces). Using asymptotic representations of the continuation of the tsunami eigenfunction into the solid Earth, we derive analytical expressions of the spectral amplitude generated by both systems. We show that the quadrupolar corrections defined by DAHLEN (1993) in the case of landslides can result in an increase of 1 to 2 orders of magnitude of the effective force. Even so, the spectrum of tsunami waves generated by landslides is found to be offset significantly to relatively high frequencies (10 mHz), where dispersion becomes important and eventually diminishes time-domain amplitudes. We proceed to calculate the total energy delivered into the tsunami modes by integrating the energy of multiplets for an average source geometry. In the case of dislocation sources, and taking into account the corner frequency of the source, we reproduce the scaling with $M_0^{4/3}$ which was derived from purely static arguments by KAJIURA (1981). We compare the directivity patterns of far-field tsunami waves by dislocations and landslides, and conclude that the latter cannot give rise to pronounced lobes of directivity for physically acceptable values of the velocity of the slide. Directivity thus constitutes a robust discriminant of the nature of the source which, when applied to the 1946 Aleutian tsunami in the far-field, requires generation by a dislocative source.

Key words: Tsumani theory, normal modes, landslides, directivity.

1. Introduction and Background

The catastrophic 1998 local tsunami in Papua New Guinea [PNG] featured characteristics which could not be modeled with a classical dislocation source, namely an excessive value of runup on the nearby coast, relative to the inferred slip on the fault plane, a peaked lateral distribution of the runup along the coast, and a significant delay of the wave at the shore. These properties suggested that the PNG tsunami was generated by an offshore underwater landslide, itself triggered with a 13-mn delay by the earthquake (e.g., SYNOLAKIS *et al.*, 2002), a model also supported by later mapping of a fresh slide using seismic reflection techniques (SWEET and SILVER, 2003).

The identification of a landslide as the source of the PNG event has led to a renewal of interest in the topic of tsunamigenic landslides, as expressed for example

[1] Department of Geological Sciences, Northwestern University, Evanston, IL 60208, U.S.A.

in this topical issue. Indeed, long before the physical representation of the earthquake source as a double-couple was first proposed by VVEDENSKAYA (1956), and the first seismic moment tensor computed from seismic waves by AKI (1966), a number of visionary scientists such as MILNE (1898), MONTESSUS DE BALLORE (1907) and GUTENBERG (1939) had proposed that large tsunamis could be, or even had to be, generated by underwater landslides. The successful modeling of the gigantic events of the 1960s and of their powerful tsunamis with double-couple sources (e.g., BEN-MENAHEM and ROSENMAN, 1972) temporarily eclipsed the importance of landslides as tsunami generators. Then, direct observation of a major aerial landslide during the 1980 explosion of Mount St. Helens led KANAMORI *et al.* (1984) to successfully model its seismic waves using single forces, and later HASEGAWA and KANAMORI (1987) and EISSLER and KANAMORI (1987) to apply this concept to the submarine cases of the 1929 Grand Banks and 1975 Hawaii earthquakes, which had generated locally destructive tsunamis. KANAMORI (1985) also speculated that the source of the 1946 Aleutian tsunami might have involved a landslide.

In this framework, it is important to assess theoretically the properties of tsunamis generated by both kinds of sources – seismic dislocations and landslides. In particular, it is crucial to understand which observable characteristics of tsunamis can be used as robust discriminants to identify the physical nature of the source.

In this study, we focus on far-field tsunamis, typically recorded at distances of several thousand km, and consider theoretically such properties as the frequency content of their amplitude spectrum, the total energy released into the tsunami wave, the azimuthal directivity of the far-field amplitude, and the scaling of such characteristics with source size. For this purpose, we use the normal mode formalism for tsunami waves, as described by WARD (1980, 1981, 1982), and further discussed by OKAL (1982a, 1988, 1990). It considers tsunamis as a special branch of spheroidal eigenmodes of a self-gravitating elastic Earth whose outermost shell is an ocean of depth h. The principal advantage of this approach is that it greatly simplifies the study of the coupling between the solid Earth and the water layer, i.e., the penetration of the tsunami eigenfunction into a substratum of finite rigidity, an approach originally found in POD"YAPOL'SKII (1970), and pursued by ALEKSEEV and GUSYAKOV (1976). It also allows the immediate computation of accurate estimates of the spectral amplitudes and energies excited into individual modes by any combination of forces, by using the classical formalism of normal mode excitation, introduced by GILBERT (1970). Finally, normal mode theory lends itself easily to the comparison of surface waves and tsunamis excited by the same seismic source.

This approach is also satisfying when considering that the alternative has traditionally involved two separate calculations utilizing inconsistent models of the ocean floor. The first step uses a homogeneous half-space of finite rigidity, but featuring no layering representative of any potential sedimentary structures and no overlying ocean, and computes the static surface displacement resulting from the

earthquake dislocation, using such codes as MANSINHA and SMYLIE's (1971) or OKADA's (1985); the second step then feeds the resulting field of vertical displacements as an initial condition into numerical codes solving the propagation of the tsunami of a water layer overlying an infinitely rigid substratum.

On the other hand, the normal mode formalism has several limitations, at least in the elementary form considered in the present paper. The most important one is that it assumes a laterally homogeneous structure, and as such, an ocean of constant depth. Similarly, it cannot handle the presence of continents, and in particular of a shoreline in the vicinity of the source. Finally, it uses the asymptotic expansion of Legendre polynomials, and as such is applicable only in the far field, i.e., at distances from the source of at least several wavelengths, or a few hundred km in the case of typical tsunamis. Nevertheless, within the framework of these limitations, it can give considerable insight into many properties of tsunami waves (WARD, 1980), and in particular it allows direct comparison with those of the familiar Rayleigh modes (OKAL, 1990), to which we will also refer regularly in the course of this study.

2. Ingredients: Modes and Sources

The Tsunami Eigenfunction in the Normal Mode Formalism

In the normal mode formalism, the tsunami wave is simply a special case of the general six-dimensional eigenfunction of a spheroidal free oscillation (of angular degree l), as described by SAITO (1967) whose notation we shall adopt. However, considerable insight can be obtained from the classical tsunami theory derived in the case of a flat-layered ocean overlying a perfectly rigid substratum; the mode-wave equivalence between the two approaches was explored by OKAL (1982a). In this particular scenario, the vertical displacement y_1 of the water varies linearly from 0 at the bottom to Y at the surface, $y_1 = Y(1 - z/h)$, the horizontal displacement eigenfunction, ly_3, is constant throughout the column, $ly_3 = Y/(hk)$, and the normal stress y_2 (the opposite of the overpressure) grows linearly from surface to bottom, $y_2 = -Y\rho_w gz/h$. In these formulae, h is the thickness of the water column, the depth coordinate z varies from 0 at the surface to h at the bottom, k is the horizontal wave number, ρ_w the density of water, and g the acceleration of gravity.

In the presence of a solid substratum of finite rigidity μ, OKAL (1988) derived the shallow structure of the eigenfunction in the solid Earth by showing that it behaves as a "pseudo-Rayleigh" wave, i.e., a combination of inhomogeneous P and S waves whose phase velocity C remains controlled by the water column and essentially unperturbed from the rigid case, while matching the overpressure $-y_2$ at the ocean floor, which is also found to be basically unchanged from the rigid case. The

displacement y_1 at the ocean floor is then controlled by the impedance of the solid at the angular frequency ω,

$$Z = \frac{y_2}{y_1} = -\mu k \frac{(2-\kappa^2)^2 - 4\sqrt{(1-\kappa^2)(1-\kappa^2/3)}}{\kappa^2\sqrt{1-\kappa^2/3}} \quad , \tag{1}$$

where $k = \omega/C = (l+1/2)/a$ is the horizontal wavenumber, and $\kappa = C/\beta$ is always much smaller than 1; β is the shear velocity of the solid, whose Poisson ratio has been taken as 1/4. In the limit $\kappa \to 0$, one has $Z \to (4/3)\mu k$ (OKAL, 1988). The vertical displacement at the ocean floor, y_1, is then given by $-Y\rho_w g/Z$, which remains much smaller than the surface displacement Y at all periods less than several hours. (By contrast, in the case of a Rayleigh mode, the boundary condition $y_2 = 0$ at the surface imposes $Z = 0$, which in turn controls the phase velocity C through the classical result $\kappa = \sqrt{2 - 2/\sqrt{3}}$.)

In essence, the weak coupling between the water and solid layers dictates the value of C (or κ), and thus Z in (1), which in turns specifies the relative amplitude of the P and S components of the pseudo-Rayleigh wave, making it easy to compute its entire structure in the substratum, including any excitation coefficients by any combination of forces (OKAL, 1988, 1990).

The Energy Integrals I_1 and I_2

Several applications such as the evaluation of the excitation coefficients of the various modes require their normalization to unit energy through the computation of the energy integrals (KANAMORI and CIPAR, 1974).

$$I_1 = \int_0^a \rho r^2 y_1^2 dr \quad \text{and} \quad I_2 = \int_0^a \rho r^2 y_3^2 dr \quad . \tag{2}$$

For Rayleigh waves, and in the limit of a wavelength much smaller than the Earth's radius ($l \gg 1$), one can approximate these integrals as:

$$I_1 = \int_0^\infty \rho_s a^2 u_z^2 dz \quad \text{and} \quad L^2 I_2 = \int_0^\infty \rho_s a^2 u_x^2 dz \quad , \tag{3}$$

where a is the Earth's radius, and u_z and u_x are the vertical and horizontal components of the displacement field of the standard Rayleigh wave of a homogeneous half-space of density ρ_s. It is straightforward to derive from (3)

$$I_1 + L^2 I_2 = 2^{1/2} 3^{3/4} Y^2 \frac{C}{\omega} \rho_s a^2 \quad , \tag{4}$$

where $L^2 = l(l+1)$. We have verified that (4) provides an acceptable approximation to the exact energy integrals; for example, for the mode ${}_0S_{100}$ ($T = 97.25$ s), it

predicts (2.75×10^{25} g*cm^2 when using $\rho_s = 3.3$ g/cm^3, and for $Y = 1$ cm) as compared to 2.5×10^{25} g*cm^2 obtained from (2) using a full normal mode eigensolution derived for the stratified spherical PREM model (DZIEWONSKI and ANDERSON, 1981). Given the crude assumptions in our model (e.g., the absence of layering, and the extension of the integrals (3) to infinity), the agreement is excellent and justifies our methodology. *For tsunami modes*, on the other hand, the integrals in (2) can be limited in practice to the water layer, where the horizontal motion is dominant in the long-wavelength approximation ($a/lh \gg 1$), leading to

$$I_1 + L^2 I_2 \approx L^2 I_2 = \rho_w \frac{a^4}{L^2 h} Y^2 = \rho_w \frac{a^2 \cdot g}{\omega^2} Y^2 \quad . \tag{5}$$

The difference in behavior with frequency of the energy in the two types of modes (ω^{-1} for Rayleigh waves, as opposed to ω^{-2} for tsunamis) is fundamental, and has important consequences on all aspects of spectral excitation by both dislocations and landslide sources.

Sources: Modeling of a Dislocation

Earthquake dislocations are modeled as double-couples of moment M_0, whose excitation of any Earth normal mode has been known since the seminal work of GILBERT (1970). We express it here for spheroidal modes in the formalism of KANAMORI and CIPAR (1974), which gives the component of vertical displacement at angular distance Δ as

$$u_r = y_1(a) M_0 \left[K_0 s_R P_l^0(\cos\Delta) - K_1 q_R P_l^1(\cos\Delta) + K_2 p_R P_l^2(\cos\Delta) \right] \cdot \cos(\omega t) \quad , \tag{6}$$

which is equivalent to a spectral amplitude in the far field (KANAMORI and STEWART, 1976)

$$|u_r(\omega)| = M_0 \frac{y_1(a)}{\sqrt{\sin\Delta}} \sqrt{\frac{\pi}{2l}} \frac{a}{U} \left| s_R K_0 - p_R l^2 K_2 - i q_R l K_1 \right| \quad . \tag{7}$$

In these formulae, a is the Earth's radius, ω its angular frequency, and U the equivalent group velocity ($U = a \cdot d\omega/dl$); P_l^m is the Legendre polynomial of degree l and order m. We refer to KANAMORI and CIPAR (1974) and KANAMORI and STEWART (1976) for the exact expressions of the excitation coefficients K_i (which depend only on frequency and source depth) and of the geometric coefficients p_R, q_R, s_R which depend only on the orientation of the dislocation relative to the Earth's surface and to the azimuth of the receiver.

As the size of the earthquake increases, source finiteness results in the saturation of spectral amplitude at any given frequency. This can be schematized across the frequency band by introducing a source spectrum characterized by a corner frequency ω_c below which interference effects are absent, and above which the source

spectrum falls off as ω^{-3} (GELLER, 1976). An estimate of the scaling of ω_c with moment M_0 is given in Appendix 1 following GELLER (1976).

Numerical values. For a large earthquake, capable of generating a transpacific tsunami ($M_0 = 5 \times 10^{28}$ dyn-cm), Equations (A9) and (A11) predict corner periods of 49 s and 130 s, for Rayleigh waves and tsunamis, respectively. These values would grow to 166 and 445 s, respectively for a mega-thrust event of the size of the 1960 Chilean earthquake ($M_0 = 2 \times 10^{30}$ dyn-cm). Furthermore, it is interesting to note the influence of the rupture velocity V_R in Equation (A7); for an earthquake with slow rupture, such as the 1992 Nicaragua "tsunami earthquake," V_R could be as slow as 1 km/s (KANAMORI and KIKUCHI, 1993), which would increase the relevant corner periods by a factor of 1.5, to as much as 200 s for the tsunami of a large earthquake (5×10^{28} dyn-cm).

We will also consider an event of the size of the PNG earthquake ($M_0 = 3.7 \times 10^{26}$ dyn-cm), which generated a mediocre far-field tsunami, reaching only decimetric amplitudes at a few Japanese harbors, and unobserved at transpacific distances.

Sources: Modeling of a Landslide

The excitation of seismic waves in the Earth by the motion of a sliding mass at its surface was modeled by KANAMORI *et al.* (1984) in the case of the massive slide accompanying the 1980 eruption of Mount St. Helens, and their model was later applied to the 1929 Grand Banks and 1975 Kalapana underwater events (HASEGAWA and KANAMORI, 1987; EISSLER and KANAMORI, 1987). It considers that the Earth is subject to the reaction of the acceleration of the sliding mass, $-M\ddot{\mathbf{x}}$. Such sources can then be represented using single forces $\mathbf{F}$ as opposed to moment tensors $\mathbf{M_0}$. However, as discussed by OKAL (1990), a major difference arises, since the source must satisfy a condition of zero impulse, which brings an additional factor ω^2 into the source time function of the landslide at low frequencies. The high-frequency behavior of a landslide is difficult to describe, since it hinges on the particular development of the initial phases of sliding, and of the braking phase of the slide at its toe. OKAL (1990) has studied theoretically several models of source time function. We will consider here the function

$$F_0(t) = F_0 \cdot [H(t) - H(t - 2\tau_1)] \cdot \sin\frac{\pi t}{\tau_1} \tag{8}$$

proposed by KANAMORI *et al.* (1984) for the Mount St. Helens eruption. Here τ_1 characterizes the duration of the source, and $H(x)$ is the Heaviside function. Relative to a step function, (8) introduces an additional spectral factor

$$X_d(\omega) = \left|\frac{\dot{F}_0(\omega)}{F_0}\right| = \left|\frac{2\omega\omega_1}{\omega^2 - \omega_1^2} \cdot \sin\frac{\omega\tau_1}{2}\right| \quad (\omega_1 = \pi/\tau_1) \ , \tag{9}$$

which can be approximated by $X_d = \pi\frac{\omega^2}{\omega_1^2}$ (small ω) and $\frac{4}{\pi}\frac{\omega_1}{\omega}$ (large ω). This amounts to defining a *"corner frequency"* ω_c where the low- and high-frequency trends intersect:

$$\omega_c = \omega_1\left(\frac{4}{\pi^2}\right)^{1/3} = 0.74\omega_1 \ . \tag{10}$$

Note that for other models of acceleration of the slump, the high-frequency spectrum may vary, but the low-frequency behavior will always be $\leq \omega^2$, in order to satisfy the zero-impulse condition.

In addition, DAHLEN (1993) has shown that the above description of a shallow landslide by a single force acting on an unperturbed elastic medium (which he termed the "Kanamori force, F_K") neglects the influence of the development of discontinuities at the ends of the sliding block, which are equivalent to a series of three quadrupolar terms. (Note a typographic error in DAHLEN's (1993) Figure 5: in the depiction of the surface quadrupoles, the first two should read " o ⊕ ⊖ o " and " ⊕ / ⊖ ", respectively.) In the formalism of OKAL (1982b), these terms contribute three second-order (three-index) moment components: $M_{\theta\theta\theta} = \frac{8}{3}\beta_0^2 MD$; $M_{\theta\phi\phi} = \beta_0^2 MD$; and $M_{\phi\theta\phi} = \frac{5}{3}\beta_0^2 MD$, with the radial axis $\hat{\mathbf{u}}_\theta$ oriented along the direction of sliding, $\hat{\mathbf{s}}$ in Dahlen's notation. Using the full set of three-index excitation coefficients derived in Equations (18) and (46) of OKAL (1982b), it is easy to verify that DAHLEN's (1993) simple correction to the Kanamori force F_K, namely the factor $f_D = \left(1 - \frac{8}{3}\frac{\beta_0^2}{C^2}\right)$, holds for tsunami modes in the limit $l \gg 1$. In this formalism, M is the mass of the sliding block, β_0 the shear velocity inside it, D the total displacement during the slide, and C the phase velocity of the relevant mode. Equation (8) can then be used to represent the landslide, with $F_0 = F_K \cdot f_D$.

A significant difference between tsunami and Rayleigh modes then arises from the difference in phase velocity C. DAHLEN (1993) was able to explain the general success of the Kanamori force in modeling such events as the Mount St. Helens landslide (for which there exists a precisely witnessed estimate of its kinematics), by noting that sliding structures are bound to be strongly brecciated, and therefore to feature low shear velocities for which the correction $\frac{8}{3}\frac{\beta_0^2}{C^2}$ becomes negligible. For example, if β_0 falls below 1 km/s, the Dahlen correction $(f_D - 1)$ becomes only -11% for a long-period Rayleigh wave with $C = 5$ km/s. However, for a tsunami mode with $C = 220$ m/s, the same material would entice $f_D = -55$, while the cohesive slumping of a crustal block ($\beta_0 = 3.5$ km/s) would lead to $f_D = -675$; note in particular that the negative values of f_D would result in a flip of phase. In real life, and for an underwater landslide, the situation is made more complex by the possible evolution of the slide into a turbidity current, in which

case the value of β_0 could be regarded as evolving with time from a finite value to essentially zero.

Numerical estimates. Given the small number of well-studied cases of underwater landslides as sources of tsunamis, it is difficult to estimate typical values of the parameters F_K, τ_1, and f_D, let alone of their scaling with the overall size of the slide. For the 1929 Grand Banks slide, HASEGAWA and KANAMORI (1987) suggested $F_K = 1.4 \times 10^{20}$ dyn, but found little resolution of the duration τ_1 of the source, which they estimated at between 25 and 90 s. For the 1975 Kalapana event, ANDO (1979) and EISSLER and KANAMORI (1987) suggested a volume $V \approx 1000\,\text{km}^3$ and a characteristic time $\tau_1 \approx 90$ s. Despite its locally catastrophic tsunami, the 1998 PNG event was considerably smaller, with $V \approx 4\,\text{km}^3$ and $\tau_1 = 22$ s (SYNOLAKIS *et al.*, 2002; SWEET and SILVER, 2003).

In this framework, and for the purpose of comparing the order of magnitude of various characteristics of tsunamis generated by dislocations and landslides, we will consider a reference landslide with a volume $V = 500\,\text{km}^3$, $\tau_1 = 60$ s, and use a Dahlen correction $f_D = -50$ for the tsunami mode ($f_D = 0.9$ for a long-period Rayleigh mode). On an ocean floor sloping 10°, these values lead to $F_K = 2.2 \times 10^{20}$ dyn (note (DAHLEN, 1993) that the true density of the sliding material, *uncorrected for buoyancy*, should be used in the excitation calculations), and $F_0 = 1.1 \times 10^{22}$ dyn for the tsunami modes; these numbers may be applicable to the underwater landslide suggested as a source of the catastrophic near-field runup of the 1946 Aleutian tsunami (FRYER and WATTS, 2000; PLAFKER *et al.*, 2002). We also consider the slide discussed theoretically by OKAL and SYNOLAKIS (2003), which is inspired by the PNG event (albeit larger). It features a considerably smaller volume than our reference slide ($10\,\text{km}^3$; $F_K = 6.8 \times 10^{18}$ dyn), but we use a larger value of the correction, $f_D = -200$, the slide having been contained in the amphitheater, and thus presumably kept a greater level of cohesion. For that smaller, "PNG-type" slide, we use a shorter characteristic time, $\tau_1 = 22$ s.

3. Average Excitation and Spectral Amplitudes

Excitation by a Dislocation

The excitation of a normal mode (seismic or tsunami) by a shallow dislocation will in general depend on the geometry of the source, but an average value can be estimated as follows. The various coefficients K_i are expressed as combinations of the components of the mode's eigenfunction (KANAMORI and CIPAR, 1974). For example,

$$K_2 = \frac{2l+1}{4\pi\omega^2[I_1 + L^2 I_2]} \cdot \frac{y_3(r_s)}{r_s} \quad , \tag{11}$$

where r_s is the distance from the seismic source to the Earth's center.

Rayleigh Waves

In the limit of a shallow source ($r_s \to a$), using (4) and the classical surface aspect ratio of the standard Rayleigh wave, $ly_3 = -0.68Y$, it is straightforward to obtain

$$K_2 \approx -0.034 \cdot \frac{Y^{-1}}{a^2 \rho_s} \cdot \frac{1}{C^2 l} \approx -\frac{0.00246}{C^2 l} \quad , \tag{12}$$

if C is in km/s, K_2 in units of 10^{-27} dyn^{-1}, and for a standard normalization ($Y = 1$ cm). We have verified that (12) provides an acceptable estimate of K_2: sub-Moho values are computed at -2.43×10^{-6} and -1.46×10^{-6}, for ${}_0S_{50}$ and ${}_0S_{100}$, respectively, as compared to -3.04×10^{-6} and -1.50×10^{-6} in the PREM model (DZIEWONSKI and ANDERSON, 1981).

The pure dip-slip coefficient, K_1, which is proportional to the eigenstress component y_4 of the mode, vanishes at the surface, and hence can be taken as 0 in Equation (6). Finally, the coefficient K_0 behaves as $-5/3 \cdot L^2 K_2$ for the Rayleigh waves of a shallow source (OKAL, 1988). We can then assume an average value of 0.46 for the trigonometric function $|(5/3)s_R + p_R|$, take $C = 4.5$ km/s and $U = 3.8$ km/s on average, to obtain an asymptotic expression of the spectral amplitude

$$|u_r(\omega)| = 0.118 l^{1/2} \frac{M_0}{\sqrt{\sin \Delta}} \quad , \tag{13}$$

where u_r is in cm*s and M_0 in 10^{27} dyn-cm. It predicts values of 1.74 cm*s at $T = 40$ s ($l = 222$) and 0.70 cm*s at $T = 250$ s ($l = 36$), for a moment of 10^{27} dyn-cm, observed at $\Delta = 90°$ in the absence of attenuation. These results are in general agreement with those obtained from the formalism of the mantle magnitude M_m (OKAL and TALANDIER, 1989) (2.04 cm*s and 0.60 cm*s, respectively), which indicates that our approximations provide adequate orders of magnitude of the scaling of spectral amplitudes with moment, despite the drastic simplifications used in the present study. Note in particular that we use constant values for C and U, in view of the fact that in the real Earth, they are slowly varying parameters in the range of frequencies considered (typically 2 to 10 mHz); we also neglect the influence that crustal layering would have on excitation coefficients.

Tsunami Modes

In the case of a tsunami mode, we use $Z = (4/3)\mu k$ and the structure of the pseudo-Rayleigh wave in the solid to infer $ly_3/y_1 \to -1/3$ at the top of the solid (OKAL, 1988 and *erratum*, 1991). Recalling (11) and (5), we obtain

$$K_2 \approx \frac{1}{8\pi\mu}\frac{Y^{-1}}{la^2}; \quad K_0 \approx L^2 K_2 \ . \tag{14}$$

We then consider a mantle source ($\mu = 7 \times 10^{11}$ dyn/cm^2), an ocean of depth $h = 5$ km ($C = U = 220$ m/s), and use an average value of 0.37 for the trigonometric coefficient $|s_R - p_R|$ to obtain

$$|u_r(\omega)| = 1.49 l^{1/2} \frac{M_0}{\sqrt{\sin\Delta}} \ , \tag{15}$$

which predicts spectral amplitudes of 28 cm*s and 15 cm*s at periods of 500 s ($l = 362$) and 1800 s ($l = 101$), respectively, for $M_0 = 10^{27}$ dyn-cm.

At this stage, an important conclusion is that the spectral amplitudes of Rayleigh waves and tsunamis excited by dislocations both grow with frequency as $\omega^{1/2}$ (under the assumption of a constant phase velocity). The difference in behavior of the energy integrals (4) and (5) is exactly compensated by the variable ratio, decaying like ω in the tsunami mode, between the horizontal motion in the solid, ly_3, and the surface amplitude of the wave, Y. Beyond the corner frequencies, the spectral amplitudes would decay as $\omega^{-5/2}$, as sketched on Figure 1. Note that this high-frequency behavior would be characteristic of a receiver feeling the full effect of saturation, i.e., lying *outside* the lobes of the directivity pattern; a slower fall-off with frequency beyond ω_c would be expected inside the lobes. Finally, we stress that, by using constant values of $C = U = \sqrt{gh}$, we neglect the effects of dispersion inherent at high frequencies in the exact expression, $C^2 = \frac{g}{k}\tanh(kh)$.

Excitation by a Landslide

As discussed for example by EISSLER and KANAMORI (1987) and OKAL (1990), the excitation of normal modes by single forces is expressed by an equation similar to (6)

$$u_r = y_1(a) F_0 \left[K_0^{SF} s_F P_l^0(\cos\Delta) + K_1^{SF} q_F P_l^1(\cos\Delta)\right] \cdot \cos(\omega t) \ , \tag{16}$$

where the coefficients K_i^{SF} are directly related to the K_j; for example, $K_1^{SF} = -r_s K_2$. For a sub-horizontal force, the first term in the bracket can be neglected, leading to

$$|u_r(\omega)| = F_0 \frac{y_1(a)}{\sqrt{\sin\Delta}} \sqrt{\frac{\pi}{2l}} \frac{a}{U} |q_F l K_1^{SF}| \tag{17}$$

or, on the average, given $\langle |q_F| \rangle = 2/\pi$,

$$|u_r(\omega)| = F_0 \frac{y_1(a)}{\sqrt{\sin\Delta}} \sqrt{\frac{2}{\pi l}} \frac{a r_s}{U} l |K_2| . \tag{18}$$

In the case of Rayleigh waves, we find

$$|u_r(\omega)| = 0.163 l^{-1/2} \frac{F_0 \cdot a}{\sqrt{\sin\Delta}} \ , \tag{19}$$

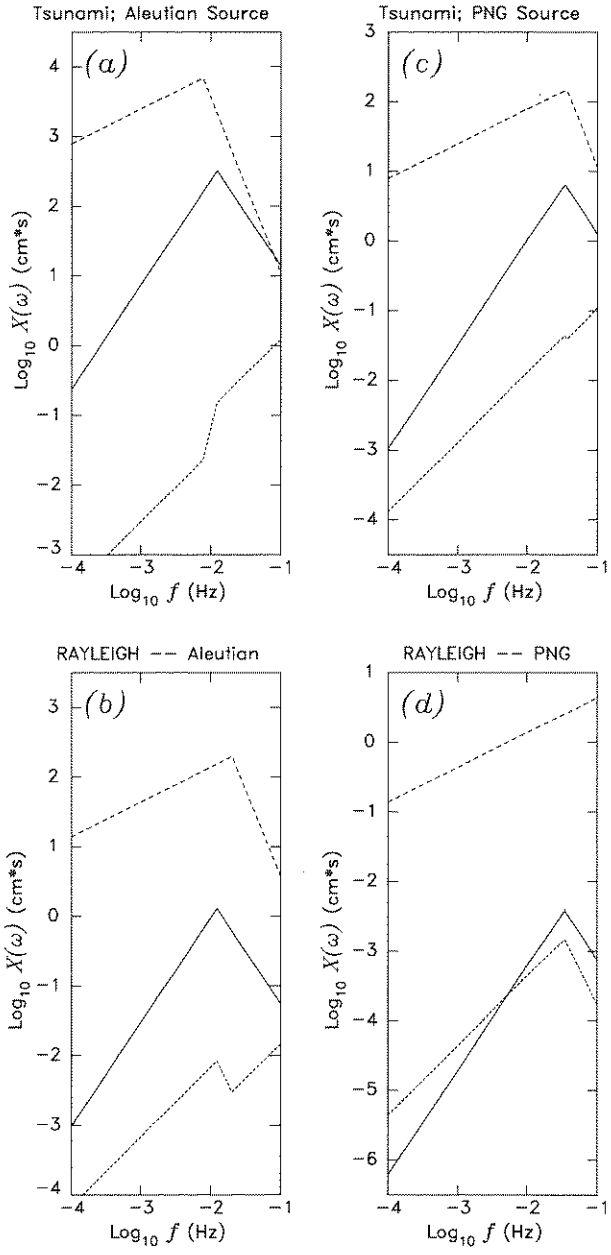

Figure 1

Comparison of the spectral amplitudes excited by simulated landslide sources (solid lines) and dislocations (dashed lines). The dotted lines are the ratios between the two. All scales are logarithmic. In the left frames, we consider the possible sources of the large 1946 Aleutian tsunami. The tsunami spectral amplitudes are shown in (*a*), the Rayleigh wave spectra in (*b*); In the right frames, we consider the PNG-type landslide source, and compare it to the dislocation source inverted by DZIEWONSKI *et al.* (1999) for the 1998 PNG earthquake. (*c*): tsunami waves; (*d*): Rayleigh waves.

where the product $F_0 \cdot a$ must be expressed in units of 10^{27} dyn*cm to obtain $u_r(\omega)$ in cm*s. The comparison of (13) and (19) suggests that the ratio of spectral amplitudes excited by a single force and a double-couple (at this stage with identical source time functions, arguably an unphysical situation) is

$$R_{SF/DC} = 1.38 \cdot \frac{1}{l} \cdot \frac{F_0 \cdot a}{M_0} \quad . \tag{20}$$

In the case of a tsunami mode, we would similarly obtain

$$|u_r(\omega)| = \frac{F_0}{\sqrt{\sin \Delta}} \sqrt{\frac{2}{\pi l}} \frac{a r_s}{U} l \frac{1}{8\pi \mu l a^2} = 3.22 l^{-1/2} \frac{F_0 \cdot a}{\sqrt{\sin \Delta}} \tag{21}$$

leading to a ratio of single-force to double-couple excitation for tsunami modes

$$T_{SF/DC} = 2.16 \cdot \frac{1}{l} \cdot \frac{F_0 \cdot a}{M_0} \quad . \tag{22}$$

In (20) and (22), the numerical coefficients 1.38 and 2.16 are smaller than computed in OKAL (1990) (2.65 and 6.00, respectively), because we have restricted ourselves to sub-horizontal forces, which are more representative of a mass movement on a shallow incline, but less efficient at exciting spheroidal modes. Note also that Equations (20) and (22) are not directly comparable, because of the different Dahlen corrections, which result in different values of F_0 for the same event.

We then invoke the appropriate source time functions for the dislocation and landslide sources, and compare the resulting spectral amplitudes on Figure 1. Frame (*a*) plots the spectral amplitudes of tsunami modes excited in the far field by the two kinds of sources proposed to model the 1946 Aleutian tsunami: a large dislocation ($M_0 = 5 \times 10^{28}$ dyn-cm) and a major landslide with a volume of 500 km^3, while Frame (*b*) presents the corresponding spectra for conventional seismic surface waves (Rayleigh). Several important results are immediately apparent:

First and foremost, the far-field tsunami amplitude of the reference landslide remains smaller than that of the dislocation by more than one order of magnitude; at frequencies typical of the observed tsunami (1 mHz), this deficiency reaches more than two orders of magnitude; the landslide would become a relatively more efficient tsunami generator only beyond the corner frequencies ($f \geq 10$ mHz), outside the realm of conventional tsunami waves and where many of our approximations break down, notably our assumption of undispersed propagation (C or U independent of frequency). In particular, the Aleutian landslide model generates a far-field tsunami whose spectral amplitudes are comparable to those of a dislocation of moment 2×10^{26} dyn-cm, a size of earthquake known not to excite detectable far-field tsunamis.

Second, in the case of the landslide, and precisely because the tsunami spectral amplitude is peaked around ω_c (i.e., around 10 mHz), and falls off fast (as $\omega^{3/2}$) at

lower frequencies, it suffers significant dispersion when propagating large distances over a deep ocean. Indeed, the dispersion $|dU(\omega)/d\omega|$ is maximum around 150 s for a 5-km deep ocean where it reaches as much as 2 km/rd. It will affect slightly the spectral amplitudes (computed for constant C on Fig. 1), but strongly the spectral phases, resulting in the dispersion of tsunami energy, and a sharp reduction in time domain amplitude. By contrast, the tsunami generated by the dislocation source falls off slower with frequency (as $\omega^{1/2}$), and thus retains significant spectral amplitude at the typical frequencies (1 mHz) where dispersion is absent, thus allowing the retention of a significant time domain amplitude.

The bottom line from these calculations is that the combination of a lesser absolute level of excitation and a more pronounced shift of the spectral energy towards higher frequencies suffering strong dispersion, makes the landslide source a significantly deficient far-field tsunami generator, as compared to a classical dislocation.

In Frame (*b*), we similarly explore the excitation of Rayleigh waves by the two sources. The similarity between Equations (13) and (15), and (19) and (21) results in comparable behavior. However, the lesser value of the Dahlen correction f_D for Rayleigh waves results in an additional deficiency of the landslide source, reaching more than two orders of magnitude across the spectrum considered (typically 5 to 10 mHz).

In the case of the smaller event, inspired from the PNG source and simulated in Frames (*c*) and (*d*), the landslide source remains undetectable in the far field (note the translation of the vertical scale between the left and right frames). Also, for this model of a supposedly more cohesive slide, there is a greater scatter in the Dahlen correction ratios ($f_D = -200$ for the tsunami; 0.5 for Rayleigh waves), as compared to the Aleutian case ($f_D = -50$ for the tsunami; 0.9 for Rayleigh waves). As a result, the relative Tsunami-to-Rayleigh efficiency of the landslide is enhanced by an additional factor of ~ 7. In conclusion, a PNG-type landslide (even taken here as substantially larger than mapped by SWEET and SILVER (2003)) would remain undetectable in the far-field: its tsunami would be 20 times smaller than that of the earthquake; the ratio would reach 300 for its Rayleigh waves. Clearly, the absence of far-field signature cannot be an argument against a landslide model for the PNG local tsunami.

We wish to emphasize that formulae such as (13), (15), (19) and (21), or their plots on Figure 1 after convolution with the respective source time functions, should not be applied in the near field, and this for several reasons. First, the spectral amplitudes in those formulae are calculated using the asymptotic expansions of the Legendre polynomials, which break down as $\Delta \rightarrow 0$, in practice within one wavelength of the source. While Equations (6) and (16) remain in principle valid, (7) and (17) do not. Furthermore, propagation in the near field occurs entirely, from source to receiver, over variable bathymetry, a structure that our approach does not handle.

4. The Energy of Tsunami Modes

In this section, we address the question of the total energy excited into tsunami modes by dislocation and landslide sources, and of its scaling with the size of the source.

The Dislocation Source

The energy of an oscillating spheroidal singlet S_l^m of the Earth can be readily computed in its kinetic form as

$$E = \frac{1}{2} \int_{\text{Earth}} \rho \dot{\mathbf{u}}^2 \, dV = \frac{1}{2} \omega^2 (I_1 + L^2 I_2) \cdot A(m) \quad , \tag{23}$$

where I_1 and I_2 were defined in (2) and the azimuthal integrals $A(m)$ are respectively,

$$A(0) = \frac{4\pi}{2l+1}; \quad A(\pm 1) = \frac{2\pi L^2}{2l+1}; \quad A(\pm 2) = \frac{2\pi L^4}{2l+1}. \tag{24}$$

To obtain the total energy excited into a multiplet, one simply adds that of the singlets (which are orthogonal on the sphere), weighted by the appropriate excitation coefficients.

- In the case of a *Rayleigh mode*, we have

$$E_{\text{multiplet}} = \frac{3^{3/4}}{2^{1/2}} \frac{\omega^2 \rho_s a^3}{l} Y^2 \cdot M_0^2 \left[A(0) c_0^2 K_0^2 + A(-1) c_{-1}^2 L^2 K_1^2 \right.$$
$$\left. + A(1) c_1^2 L^2 K_1^2 + A(-2) c_{-2}^2 L^4 K_2^2 + A(2) c_2^2 L^4 K_2^2 \right] \quad . \tag{25}$$

Here, the coefficients c_i are variations of s_R, q_R and p_R. They do not vary independently, but their average value for all focal mechanisms is on the order of 1/3. In first approximation, we can neglect the $m = \pm 1$ terms in (25), since K_1 vanishes asymptotically at the surface. Noting that $K_0 = -(5/3) L^2 K_2$ at the surface of a Poisson solid (OKAL, 1990), and substituting (12) and (24), we find the energy of a spheroidal multiplet as

$$E_{\text{multiplet}}^{\text{Rayleigh}} = N \frac{1}{a^3 C^2 \rho_s} \cdot L^2 M_0^2 \quad , \tag{26}$$

where the non-dimensional constant N has the approximate value 4.8×10^{-3}. This energy of a single multiplet is, as expected (WARD, 1980), proportional to the *square* of the excitation M_0, and for a constant phase velocity C, grows as ω^2.

- In the case of a *Tsunami*, we need to replace the expression of the integrals I_1 and I_2 with (5), substitute $K_0 = L^2 K_2$, and use Equation (14) to approximate K_2 as a function of ω. The result is

$$E_{\text{multiplet}}^{\text{Tsunami}} = \frac{1}{288\pi} \cdot \frac{\rho_w g}{\mu a^2} \cdot l \cdot M_0^2 \ . \tag{27}$$

The comparison of (26) and (27) reaffirms the fundamental difference noted above, namely that the tsunami energy grows as ω, rather than ω^2. In other words, for the same dislocation source, the tsunami branch will be lower-frequency or more "red" than the Rayleigh wave†.

Integration over Frequency

There remains to integrate (26) and (27) over frequency to obtain the total energy carried by the Rayleigh and tsunami waves, replacing summation over l by integration over ω (weighted by a/U), and taking into account the source time function of the dislocation. The total energy for the branch becomes:

$$E = a \cdot \left[\int_0^{\omega_c} \frac{1}{U} E_{\text{multiplet}}(\omega) d\omega \quad + \quad \int_{\omega_c}^{\infty} \frac{1}{U} E_{\text{multiplet}}(\omega) \frac{\omega_c^6}{\omega^6} d\omega \right] \ , \tag{28}$$

where, as a further approximation, the integration bounds are extended to zero and infinite frequencies, on account of the characteristics of the source functions. Assuming that U and C can be taken as constant, we find

$$E^{\text{Rayleigh}} = 3.2 \times 10^{-3} \frac{1}{UC^4 \rho_s} \omega_c^3 M_0^2; \quad E^{\text{Tsunami}} = 8.3 \times 10^{-4} \frac{\rho_w g}{UC\mu^2} \omega_c^2 M_0^2 \ . \tag{29}$$

Note that the legitimacy of carrying the integral (28) to infinite frequency could be questioned, since our simplifying assumptions (e.g., constant C) would clearly break down as $\omega \to \infty$. However, the sharp fall off of the integrand with frequency ensures that the energy is almost entirely concentrated near ω_c, with $\omega < 2.15\omega_c$ contributing 90% of the second term of (28) (95% of the full energy integral), and thus rendering largely irrelevant any limitations on our assumptions at still higher frequencies.

After substituting the expression of the corner frequency (A8), we obtain the final result for Rayleigh waves:

$$E^{\text{Rayleigh}} = 0.055 \frac{1}{\kappa^3 \eta} \varepsilon_{\max} M_0 = 0.084 (\varepsilon_{\max} \cdot M_0) \ , \tag{30}$$

where η is the ratio of the group velocity U of the wave to the shear velocity, which we take as slightly lower than κ ($\eta = 0.85$), and $\varepsilon_{\max}$ the strain release during the rupture (see Appendix). Since $(\varepsilon_{\max} \cdot M_0)$ represents the mechanical energy released at

† Note that there is no inconsistency between the fact that the energy in the two types of waves behaves differently with frequency while spectral amplitudes have the same dependence, for the latter is a local property of the eigenfunction at the surface of the Earth, while the former involves its integral over depth.

the source by the dislocation, we come to the simple conclusion that the energy channeled into the fundamental Rayleigh branch scales directly with M_0, and represents a constant fraction, about 8%, of the total seismic energy released by the source.

The situation is quite different in the case of the tsunami wave. Substituting (27), we obtain

$$E^{\text{Tsunami}} = 5.5 \times 10^{-3} \frac{\rho_w}{\rho_s} \cdot \left(\frac{g \rho_s}{h^2 \mu^2} \right)^{1/3} \varepsilon_{\max}^{2/3} \cdot M_0^{4/3} \approx 1.04 \times 10^{-16} M_0^{4/3} \qquad (31)$$

if M_0 is in dyn-cm and E in ergs. For the reference Aleutian event, we find $E^{\text{Rayleigh}} = 4.2 \times 10^{23}$ ergs, and $E^{\text{tsunami}} = 1.9 \times 10^{22}$ ergs, or 0.4% of $(\varepsilon_{\max} \cdot M_0)$. For the smaller PNG event, these numbers would be 3.1×10^{21} ergs, 2.8×10^{19} ergs, and 0.08%, respectively. Note that the integrand in (28) falls off like ω^5 for $\omega \to \infty$, as opposed to ω^4 for Rayleigh waves. The question of the extension of (28) to infinite frequencies becomes even more irrelevant.

The energy of the tsunami is found to grow faster than M_0, which means that the fraction of released seismic energy which is channeled into the tsunami, itself grows like $M_0^{1/3}$, in other words scales like the linear dimension of the seismic source, L_f. This result agrees with OKAL and SYNOLAKIS' (2003), who used a simple model of the deformation of a rigid ocean floor to infer that the energy available to the tsunami would grow as the fourth power of the scaling dimension of a dislocation. Similarly, the scaling of E with $M_0^{4/3}$ was mentioned by AIDA (1977) and a full model derived by KAJIURA (1981), on the basis of the scaling of the static deformation of a homogeneous half-space by a seismic dislocation. Equation (31) can be directly compared to Kajiura's formula (12)

$$E_{\text{Kaj}} = \frac{1}{2} \frac{\rho_w g}{\mu^2} \alpha^{2/3} M_0^{4/3} F_{\text{Kaj}}.(\delta_f, \lambda, H, R) = \frac{1}{2^{4/3}} \frac{\rho_w g}{\mu^{4/3}} \varepsilon_{\max}^{2/3} M_0^{4/3} F_{\text{Kaj}} \ , \qquad (32)$$

where the function $F_{\text{Kaj}}.$ is a non-dimensional average of the square of the vertical deformation of the ocean bottom, scaled to the seismic slip on the fault, which depends on the geometry of faulting (dip angle δ_f and slip angle λ), on source depth H, and on the aspect ratio of the faulting area, $R = W/L_f$. Finally, in Equation (32), α is the ratio of M_0 to $S^{3/2}$, or $2^{-1/2} \mu \varepsilon_{\max}$ for a fault with $R = 1/2$ (see Appendix, Equation A4). The comparison of Equations (30) and (32) shows that our approach based on normal mode theory upholds KAJIURA's (1981) Equation (12), for an average value $F_{\text{Kaj}}. = 0.57$ in the case of a 5-km deep ocean. However, this value is about 5 times larger than its maximum proposed by Kajiura (0.11). An additional shortcoming is that the expression of E^{Tsunami} in (32) is expected to depend on the ocean depth h (varying like $h^{-2/3}$), while KAJIURA's (1981) does not. We will show below that a minor refinement to our approach, namely taking into account the finite depth penetration of the source, resolves this latter discrepancy.

The growth of E^{Tsunami} as $M_0^{4/3}$ could appear as a paradox, especially since it would predict that for large enough earthquakes, the energy of the tsunami could become greater than the total elastic energy released during the earthquake, which grows only as M_0. However, it can be verified that this would occur for an earthquake of moment 9×10^{35} dyn-cm, which in turn would scale to a fault length $L_f = 37,000$ km; the latter, approaching the Earth circumference, would obviously violate the scaling laws upon which our discussion is based. Even the 1960 Chilean earthquake, at 2×10^{30} dyn-cm the largest seismic event ever measured, would channel only 1.3% of its released energy into its far-field tsunami. The physical origin of the paradox lies in the fact that a characteristic length in the problem, namely the ocean depth h, does not scale with the source. Finally, the scaling with $M_0^{4/3}$ is also close to the behavior suggested by WARD (1982) ($M_0^{1.5}$), based on an empirical fit of published parameters such as fault length L_f and rise time τ as a function of M_0.

The Landslide Source

To compute the energy of a normal mode excited by a landslide, we simply replace, in the second line of Equation (25), the average excitation of a double-couple with that of a single force:

$$F_0^2 \cdot \left[A(0) s_F^2 K_0^2 + A(-1)(c_{-1}^{SF})^2 L^2 (K_1^{SF})^2 + A(1)(c_1^{SF})^2 L^2 (K_1^{SF})^2 \right] . \tag{33}$$

For a sub-horizontal force, the first term in the bracket is negligible, the coefficients $c_{\pm 1}^{SF}$ are, on the average, $1/\pi$ (note that they differ from their double-couple counterparts in (25)), and $K_1^{SF} \approx -aK_2$. This leads to the energy of a multiplet:

$$E_{\text{multiplet}}^{\text{Rayleigh}} = 0.0012 \frac{F_0^2}{\rho_s a C^2}; \quad E_{\text{multiplet}}^{\text{Tsunami}} = 5 \times 10^{-4} \frac{\rho_w g}{\mu^2} \cdot \frac{1}{l} \cdot F_0^2 , \tag{34}$$

which must then be integrated over frequency after weighting by the square of the appropriate source time function (10). In the case of Rayleigh waves,

$$E^{\text{Rayleigh}} = 0.0012 \frac{F_0^2}{\rho_s a C^2} \cdot \frac{a}{U} \left[\int_0^{\omega_c} \pi^2 \frac{\omega^4}{\omega_1^4} d\omega + \int_{\omega_c}^{\infty} \frac{16}{\pi^2} \frac{\omega_1^2}{\omega^2} d\omega \right] = 0.018 \cdot \frac{1}{\rho_s U C^2} \frac{(F_0^R)^2}{\tau_1} \tag{35}$$

and in the case of a tsunami,

$$E^{\text{Tsunami}} = 5 \times 10^{-4} \frac{\rho_w g}{\mu^2} \cdot F_0^2 \cdot \frac{a}{U} \left[\int_0^{\omega_c} \frac{\pi^2}{l} \frac{\omega^4}{\omega_1^4} d\omega + \int_{\omega_c}^{\infty} \frac{16}{\pi^2 l} \frac{\omega_1^2}{\omega^2} d\omega \right] \approx 0.0011 \frac{\rho_w g}{\mu^2} \cdot (F_0^T)^2 , \tag{36}$$

where we have introduced superscripts ^{R} and ^{T} on F_0 to emphasize that its values in (35) and (36) differ, due to the Dahlen corrections. In the case of the Aleutian slide, we find energies of 5.7×10^{19} and 1.5×10^{21} ergs, for the Rayleigh and tsunami waves, respectively (we use a crustal value, 3×10^{11} dyn/cm^2, for μ). In the case of the smaller, PNG-type source, we find values of 4.7×10^{16} (Rayleigh) and 2.2×10^{19} ergs (tsunami).

Scaling with Slide Dimensions

We first note that, in the case of the smaller slide, the value computed above is significantly smaller than calculated ($E_{OS} = 8 \times 10^{20}$ ergs) from simple deformation arguments by OKAL and SYNOLAKIS (2003). The two figures can however be reconciled by noting that while (36) assumes a 5-km deep ocean, E_{OS} uses a shallower water column, $h = 1500$ m in the PNG epicentral area. Although neither Equation (36) nor OKAL and SYNOLAKIS' (2003) energy estimate expressly involve h, both do indirectly, through the Dahlen correction in the former and through the dynamic response of the water column, $\alpha = v^2/2C^2$ in the latter. When the deeper value $h = 5$ km is used, the estimate E_{OS} decreases to 7.2×10^{19} ergs, only three times the modal value. This discrepancy is not unexpected, since E_{OS} computes the infusion of energy into the initial condition of the gravitational wave, whereas the modal approach is expected to break down in the near field. Indeed, it is possible to explore theoretically the ratio between the full expressions of the two estimates of the energy generated by the landslide, assuming a similar average depth of the ocean:

$$\frac{E^{\text{Tsunami}}}{E_{OS}} = \frac{0.0011 \frac{\rho_w g}{\mu^2} \left[\rho_s S_s(\delta H) \cdot g \sin\theta \cdot \frac{8}{3}\frac{\beta_0^2}{C^2}\right]^2}{\rho_w g S_s (\delta H)^2 \cdot \frac{v^4}{4C^4}} = 0.03 \frac{g^2 \sin^2\theta}{v^4} S_s \approx \frac{1}{8}\frac{S_s}{D_a^2} \quad , \qquad (37)$$

where S_s is the surface area of the slide, θ its dip angle, and v the average velocity at which the material moves. The RHS of Equation (37) is obtained by taking v as half the maximum velocity $v_{\max}$ reached during the sliding (OKAL and SYNOLAKIS, 2003), which is approximately given by $v_{\max}^2 = 2gz$, where z is the total drop of the slide. In turn, z is approximately $D_a \tan\theta$, where D_a is the horizontal distance over which the material is accelerated. Note that, in general, D_a is only a fraction of the total length traveled, D, since acceleration stops when the slide encounters a flat bottom. Finally, we take $\cos\theta = 1$ for typical shallow-dipping slides. We conclude that a difference between E^{Tsunami} and E_{OS} is predictable from the aspect ratio of the area of the slide, and the number of slide lengths traveled during the motion: $E^{\text{Tsunami}}/E_{OS} = \frac{1}{8}(W/L_f) \cdot (L_f/D_a)^2$.

Finally, we consider the scaling of the tsunami energy (36) to the total change in potential energy ΔW resulting from the sliding. The latter drops a mass of ocean floor $\rho_s S_s(\delta h)$ a vertical distance z, and replaces it with water of density ρ_w. Hence

$\Delta W = (\rho_s - \rho_w) g z S_s(\delta h)$, and the tsunami efficiency of the slide, i.e., the fraction of the released potential energy channeled into the far-field tsunami is thus:

$$\frac{E^{\text{Tsunami}}}{\Delta W} = 7.8 \times 10^{-3} \cdot \frac{\rho_w}{\rho_s - \rho_w} \cdot \sin\theta \cdot \frac{S_s(\delta H)}{h^2 z} \quad . \tag{38}$$

In the case of the PNG slide, we take an average water depth of 1.5 km, a vertical drop of 1 km, and $\theta = 15°$, to obtain an efficiency of 0.9%; in the case of the Aleutian reference slide, with an average water depth of 3 km, and a vertical drop of 6 km (to the bottom of the Aleutian trench), along a 10° slope, we find a very similar value of 1.25% for the tsunami efficiency.

These numbers are significantly greater than their counterparts for dislocation sources, and thus landslides are found to be relatively more efficient than earthquakes at partitioning their total available energy into the far-field tsunami. This is not surprising, since the landslide occurs in the water in the first place, as opposed to the dislocation, which is released inside the elastic solid Earth. However, even large landslides release less total potential energy than do earthquakes, so that their absolute levels of far-field tsunami energy are no match for that of large dislocation sources.

5. The Influence of Depth

Until now, we have assumed in all our computations that the excitation coefficients K_i could be approximated by their asymptotic values as the centroid depth $a - r_s$ goes to zero. In particular, we have regarded as negligible the pure dip-slip coefficient K_1. However, when considering large earthquakes under our scaling model, the fault width W is expected to scale as $M_0^{1/3}$, and thus the vertical extent of the source can no longer be neglected. As the K_i's are themselves function of depth, their dependence will affect the growth of excitation with earthquake size, and this property must be analyzed carefully. Note, however, that this kind of correction is not warranted for landslides sources, which never penetrate the deep Earth, since their thickness is limited to at most a few km by the stratigraphic structure of the ocean floor.

Consider a source of finite depth, extending from the surface to a depth $H = W \sin\delta_f$, where δ_f is the dip of the fault. On the average, $H = 2W/\pi$, and thus H scales with source size as:

$$H = \frac{4^{1/3}}{\pi} \frac{M_0^{1/3}}{(\mu \varepsilon_{\max})^{1/3}} \quad . \tag{39}$$

All that is needed in principle is to replace the K_i's in Equation (25) by their values averaged over the vertical extent of the source: $\bar{K}_i = \frac{1}{H} \int_0^H K_i \cdot dz$.

Rayleigh Waves

We write the seismic displacement at any depth, $u_x = ly_3$, as the sum of its components in the inhomogeneous P and S waves making up the Rayleigh wave:

$$u_x = ly_3 = Ae^{-\omega\gamma z} + Be^{-\omega\delta z} \quad , \tag{40}$$

where the values $A = -1.6119\ Y$; $B = 0.9306\ Y$; $\gamma = 0.8475/C$; $\delta = 0.3933/C$ are obtained from elementary Rayleigh wave theory for a homogeneous half-space. It is straightforward to derive, for example, a correction Φ_2 to the coefficient K_2

$$\Phi_2 = \frac{1}{A+B}\bar{u}_x = \frac{1}{(A+B)H\omega} \cdot \left[\frac{A}{\gamma}(1 - e^{-\omega\gamma H}) + \frac{B}{\delta}(1 - e^{-\omega\delta H})\right] \tag{41}$$

which is used to replace K_2 in (25) with

$$\bar{K}_2 = K_2\Phi_2 = -0.0034\frac{Y^{-1}}{a_2\rho_s} \cdot \frac{1}{C^2 l}\Phi_2 \quad . \tag{42}$$

A similar expression could be derived for the coefficient $\bar{K}_0$, and a finite value (going to zero for $H \to 0$) for $\bar{K}_1$. The resulting energy of the multiplet is then substituted into (28) for the integration over frequency. For the low-frequency part of the spectrum, the various integrals are merely exponential functions, and the computation is easy. For example, the term involving K_2 will be

$$E_{lf(2)} = (0.0034)^2 \frac{1}{(A+B)^2}\frac{2^{1/2}\pi}{3^{5/4}}\frac{M_0^2}{C^4 U H^2} \cdot \int_0^{\omega_c} \left[\frac{A}{\gamma}(1 - e^{-\omega\gamma H}) + \frac{B}{\delta}(1 - e^{-\omega\delta H})\right]^2 \cdot d\omega \quad . \tag{43}$$

The details of the computation, available from the author on request, are of little interest; note however that since H scales with the seismic source, the product $H \cdot \omega_c/C = \xi_c \approx 1.38$ remains invariant with M_0. As such, the various exponentials in the coefficient Φ_2 (41) are always integrated to a *constant argument*, e.g., $-\omega_c\gamma H = -1.17$; $-2\omega_c\delta H = -1.09$; this property stems from the trivial observation that the corner frequency scales inversely to the linear dimension of the source. As a result, all integrals of the exponentials in (43) are proportional to Y^2/H, and $E_{lf(2)}$ scales as M_0^2/H^3, or M_0. As for the high-frequency part of the spectrum, it requires the computation of the exponential integrals

$$\mathbf{E}_\zeta(x) = \int_1^\infty t^{-\zeta} e^{-xt}\, dt \quad (\zeta = 6) \quad , \tag{44}$$

(e.g., ABRAMOWITZ and STEGUN, 1965; p. 228), all arguments x being constants of the type $\omega_c\gamma H$, which are invariant under scaling of the source. The end result is that the corrected value of the energy excited into the Rayleigh wave can be written as:

$$E^{\text{Rayleigh}} = 0.0162\frac{M_0}{\rho_s UC}(\mu\varepsilon_{\max}) = \frac{0.0162}{\kappa\eta}(M_0 \cdot \varepsilon_{\max}) = 0.0207(M_0 \cdot \varepsilon_{\max}) \ . \qquad (45)$$

We conclude that taking into account the finite depth of the source does not alter the scaling of energy with moment, but merely amounts to cutting the fraction of energy excited into the Rayleigh wave by a factor of 4. This number is not unreasonable, given that, at the corner frequency where spectral amplitude is maximum, the vertical extent of the fault is on the order of 0.5 to 1.2 skin depths of the shear and compressional potentials, respectively, so that the amplitude of the eigenfunctions is cut on the average by a factor exp(0.8) = 2.2; the energy should be cut by a factor of about 5, but some gain is achieved by allowing a contribution from the dip-slip coefficient K_1.

Tsunamis

The computation in the case of a tsunami proceeds in a conceptually similar fashion. For example, the structure of the pseudo-Rayleigh wave in the half-space leads to

$$u_x = ly_3 = \frac{\rho_w g}{\mu k} \cdot \left(A_3 e^{-\omega\gamma z} + B_3 e^{-\omega\delta z}\right) \ , \qquad (46)$$

the coefficients A_3 and B_3 being now

$$\begin{aligned} A_3 &= -\frac{2-\kappa^2}{(2-\kappa^2)^2 - 4\sqrt{1-\kappa^2}\sqrt{1-\kappa^2/3}} \cdot Y; \\ B_3 &= \frac{2\sqrt{1-\kappa^2}\sqrt{1-\kappa^2/3}}{(2-\kappa^2)^2 - 4\sqrt{1-\kappa^2}\sqrt{1-\kappa^2/3}} \cdot Y \end{aligned} \qquad (47)$$

and the skin depth coefficients

$$\gamma = \frac{\sqrt{1-\kappa^2/3}}{C}; \qquad \delta = \frac{\sqrt{1-\kappa^2}}{C} \ . \qquad (48)$$

An additional difficulty arises in the limit $\kappa \ll 1$ (typically $\kappa = 0.06$ for tsunamis) since both A_3 and B_3 are of order κ^{-2}, and hence a formulation such as (46) consists of subtracting two very large terms to find their finite difference, a notoriously unstable computational procedure. Nevertheless, the careful expansion of (46) in the vicinity of $\kappa \to 0$ can yield important results.

The deep point source double-couple. Before examining the influence of finite depth penetration on the generation of tsunami energy by a shallow dislocation source, we address the more general question of the variation of tsunami excitation with depth by a point source double-couple. This is an important matter, since it has often been assumed that only the shallowest sources, namely within a few km of the ocean floor, can excite significant tsunamis, including in the far field.

While the representation (46) is similar to the case of standard Rayleigh waves, we note that since $\kappa = C/\beta \ll 1$, both γ and δ are close to $1/C$, and both potentials (as well as all combinations thereof, including excitation coefficients) decay with depth essentially as $e^{-\omega z/C}$. This means that the skin depth of the pseudo-Rayleigh wave is comparable to the wavelength of the tsunami, typically hundreds of km. As a consequence, tsunami excitation in the far field is not significantly decreased in the first few tens of km inside the Earth. This result was obtained by OKAL (1988) on the basis of the computation of individual normal mode solutions (his Fig. 7), but was not previously rationalized theoretically. Although arguably not intuitive, it explains the generation of tsunamis detectable in the far field by intermediate depth earthquakes, such as the Tonga event of 22 June 1977 (TALANDIER and OKAL, 1979; LUNDGREN and OKAL, 1988).

In particular, the contribution of the K_2 terms to the energy of a multiplet excited by a point-source double-couple at depth z is then

$$E_{\text{multiplet}(2)} = \frac{1}{36\pi} \cdot \frac{M_0^2}{Y^2} \cdot \frac{\rho_w g}{a^2 \mu^2} \cdot l \cdot \left(A_3 e^{-\omega\gamma z} + B_3 e^{-\omega\delta z}\right)^2 \quad . \tag{49}$$

This formula generalizes (27) to any focal depth z. (Note that if $z \to 0$, the bracket in (49) goes to $Y^2/16$, leading to a constant $1/(576\ \pi)$, which is half that in (27), since we have not accounted for the K_0 terms.)

The shallow source extending at depth. We proceed to average (49) (and similar terms emanating from K_0 and K_1) over depth (z ranging from 0 to H), and then to integrate over frequency, leading to

$$E_{lf(2)} = \frac{M_0^2}{36\pi} \cdot \frac{\rho_w g Y^{-2}}{\mu^2 UCH^2} \int_0^{\omega_c} \frac{1}{\omega} \left(\frac{A_3}{\gamma} \left(1 - e^{-\omega\gamma H}\right) + \frac{B_3}{\delta} \left(1 - e^{-\omega\delta H}\right) \right)^2 d\omega \tag{50}$$

as the low-frequency ($\omega < \omega_c$) part of the K_2 terms of the energy integral. When comparing this expression with (43), note the additional factor $1/\omega$ in the integrand. It leads to a more complex set of exponential integrals of the form

$$\mathbf{I}_{a,b}(\xi) = \int_0^{\xi} \frac{(1 - e^{-at})(1 - e^{-bt})}{t} dt \quad . \tag{51}$$

Specifically, the integral in (50) is a sum of terms of the form $\frac{A'A''}{\gamma'\gamma''} \mathbf{I}_{C\gamma',C\gamma''}(\xi_c)$ where A' and A'' are either A_3 or B_3 (given in (47)), and γ' and γ'' either γ or δ (given by (48)), and the variable $\xi_c = \omega_c H/C$ is invariant upon scaling of the source (note that its value is larger in the case of a tsunami ($\xi_c \approx 9.8$) than for a Rayleigh wave). The leading terms in (50) can be evaluated by expanding A_3, B_3, γ, and δ in the vicinity of $\kappa = 0$. It is found that the integral in (50) is equivalent to

$$\frac{1}{16} \cdot C^2 Y^2 \cdot \left[\mathbb{I}_{1,1}(\xi_c) - 1 \right] \ . \tag{52}$$

When the other terms (governed by K_0 and K_1) are included, the total low-frequency part of the integral adds to:

$$E_{lf} = \frac{M_0^2}{36\pi} \cdot \frac{\rho_w g C}{\mu^2 U H^2} \left[\frac{33}{8} \mathbb{I}_{1,1}(\xi_c) - \frac{23}{8} \right] \ . \tag{53}$$

As for the high-frequency part of the energy, it takes the form (again written for the K_2 terms only):

$$E_{hf(2)} = \frac{M_0^2}{36\pi} \cdot \frac{\rho_w g Y^{-2}}{\mu^2 U C H^2} \int_{\omega_c}^{\infty} \frac{1}{\omega} \frac{\omega_c^6}{\omega^6} \left(\frac{A_3}{\gamma} \left(1 - e^{-\omega \gamma H} \right) + \frac{B_3}{\delta} \left(1 - e^{-\omega \delta H} \right) \right)^2 d\omega \ . \tag{54}$$

In principle, this amounts to a combination of exponential integrals $\mathbb{E}_7(x)$ whose arguments x are combinations $\omega_c H \gamma'$ and $\omega_c H(\gamma' + \gamma'')$. Careful expansion near $\kappa \to 0$ shows that the leading term of the integral in (54) is

$$\frac{1}{6} \left(\frac{A_3}{\gamma} + \frac{B_3}{\delta} \right)^2 \underset{\kappa \to 0}{\approx} \frac{C^2 Y^2}{96} \ . \tag{55}$$

When the K_0 and K_1 terms are included, this expression becomes (33/48) $C^2 Y^2$, and the total energy of the tsunami wave (replacing Equation (31)):

$$E = \frac{M_0^2}{36\pi} \cdot \frac{\rho_w g}{\mu^2 H^2} \cdot \left[\frac{33}{8} \mathbb{I}_{1,1}(\xi_c) - \frac{35}{16} \right] \ . \tag{56}$$

It still formally depends on the ocean depth h through the variable $\xi_c = \frac{(28/5)^{1/3}}{(2\pi)^{1/6}} \kappa^{-2/3}$, which would vary from 9.8 for $h = 5$ km, to 14.5 for $h = 1500$ m. The corresponding values of $\mathbb{I}_{1,1}$, computed by expanding the integral into an alternating series, are 2.08 and 2.56, suggesting only a minor dependence. We then obtain for the 5-km ocean:

$$E = 6.328 \frac{M_0^2}{36\pi} \cdot \frac{\rho_w g}{\mu^2 H^2} = 0.219 \frac{\rho_w g}{\mu^{4/3}} \cdot \varepsilon_{\max}^{2/3} \cdot M_0^{4/3} \approx 7.4 \times 10^{-17} M_0^{4/3} \tag{57}$$

if M_0 is in dyn-cm and E in ergs. With respect to Equation (31), depth averaging results in a correction of only 30%, which is explained by the generally slower decay of the eigenpotentials with depth, as compared to Rayleigh waves. Note in particular that E no longer formally depends on the depth h of the oceanic column, because of the slow variation of $\mathbb{I}_{1,1}$ in the range of values considered. We can regard (57) as the final expression of the energy of a far-field tsunami generated by a dislocation of moment M_0, as predicted by normal mode theory.

It is rather difficult to assess the accuracy of this formula, because there does not exist, to our knowledge, a universal experimental method for measuring the energy of large transoceanic tsunamis. As summarized by IIDA (1963), various methods have

been used in this respect, which fall basically into two categories: (i) attempts at integrating backwards to the source the kinetic energy flux estimated from tidal gauge records at distant stations; and (ii) using some form of scaling law relating tsunami energy to earthquake magnitude. Obviously, only (i) can be considered an independent physical measurement of the energy of the tsunami wave. On Figure 2, we compare the values predicted by (57) to those reported by IIDA (1963) as having been obtained following (i). The large scatter reflects the poor quality of those measurements, which likely included near-field observations, and could have been affected by site response at far-field tidal gauge stations.

A more remarkable result is the total similarity of the corrected expression (57) with KAJIURA's (1981) formula (12) (see Equation (32)), which he obtained from the computation of a purely static deformation field. In this respect, the present derivation represents an interesting example of the power of the normal mode formalism to directly handle the coupling between liquid ocean and solid Earth. On the other hand, the corresponding value of F_{Kaj}. equivalent to (57) remains too high.

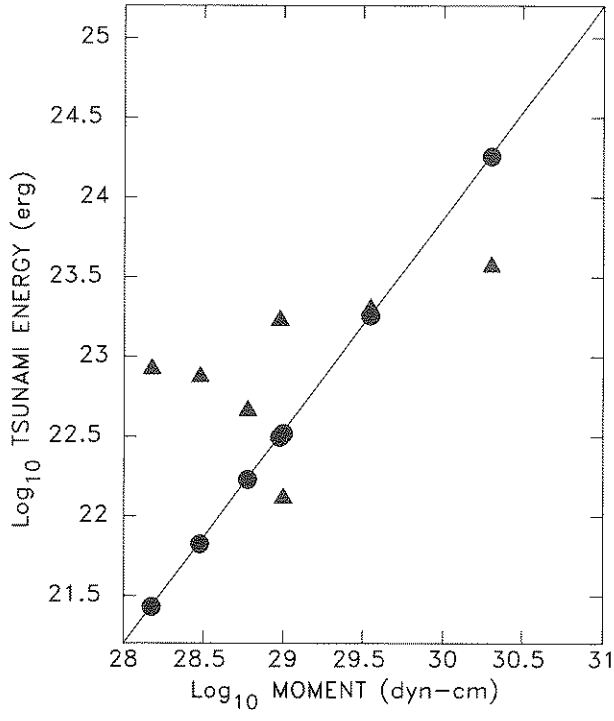

Figure 2
Comparison of values of tsunami energy obtained from (57) with estimates identified by IIDA (1963) as obtained from energy flux computations. Only those events for which a seismic moment is available in the literature (KANAMORI, 1972b; OKAL, 1992) are used. The energy values resulting from (57) are plotted as solid dots; values reported by IIDA (1963) are shown as triangles.

6. Directivity

We examine here in very general terms the directivity patterns of tsunamis generated by both dislocations and landslides. We recall that the azimuthal dependence of the amplitude radiated by a seismic source – dislocation or landslide – is affected both by the orientation of the source (resulting in the preferential excitation of the various azimuthal orders m in (6)), and by the spacio-temporal evolution of the position of the source. The former, called *radiation pattern*, is a point-source property; the latter, called *directivity* is rooted in the finite dimension of the source. We refer to BEN-MENAHEM (1961) for the definition of the directivity function DIR generated by a source of length L_f, moving at a velocity V_R ("rupture velocity") in the azimuth ϕ from the direction of observation in the far field:

$$DIR(\phi) = \frac{\sin X}{X}; \qquad X = \frac{\omega L_f}{2C} \cdot \left(\frac{C}{V_R} - \cos \phi \right) . \tag{58}$$

The parameter DIR is to be multiplied into the spectral amplitude predicted in the azimuth ϕ, as given by (7) or (17). Its expression results from the simple decomposition of the moving source into an integral of elementary sub-sources along its path in space and time. Note that $DIR = 1$ over an appreciable range of frequencies requires $X = 0$.

In order to develop a significant directivity pattern, two conditions are necessary in (58). First, the ratio $\omega L_f / V_R$ must be large, in other words the duration of the source, L_f / V_R must be at least comparable to the period of the wave; otherwise the source can be regarded as instantaneous, and all values of X are small, regardless of ϕ. Second, the values of X must change significantly with the azimuth ϕ, which excludes the case $C \gg V_R$. These simple remarks lead to fundamentally different regimes, depending on the ratio V_R/C, which have fundamental application to tsunamigenic events.

* *If the rupture is "sonic,"* i.e., V_R comparable to C, then (58) is maximum for $\cos \phi \approx 1$ or $\phi \approx 0$: in the direction (and sense) of rupture, the interference between all elements of the source is constructive and the amplitude maximum. This is the classical case of seismic surface waves from large earthquakes featuring conventional rupture, for which $C \approx V_R \approx 3.5$ to 4 km/s (Figure 3a).

* *If the rupture is hypersonic*, i.e., $V_R \gg C$, then $X = 0$ has the exact solution $\cos \phi = C/V_R \ll 1$, essentially at right angles from the rupture. This is the case of tsunamis generated by large seismic dislocations (typically, $V_R/C = 15$), as first exemplified by BEN-MENAHEM and ROSENMAN (1972) in the case of the 1964 Alaskan earthquake. OKAL and TALANDIER (1991) later discussed the width of the directivity lobes and concluded that tsunamis had generally much narrower lobes than the mantle waves generated by the same dislocations, as illustrated on Figure 3b.

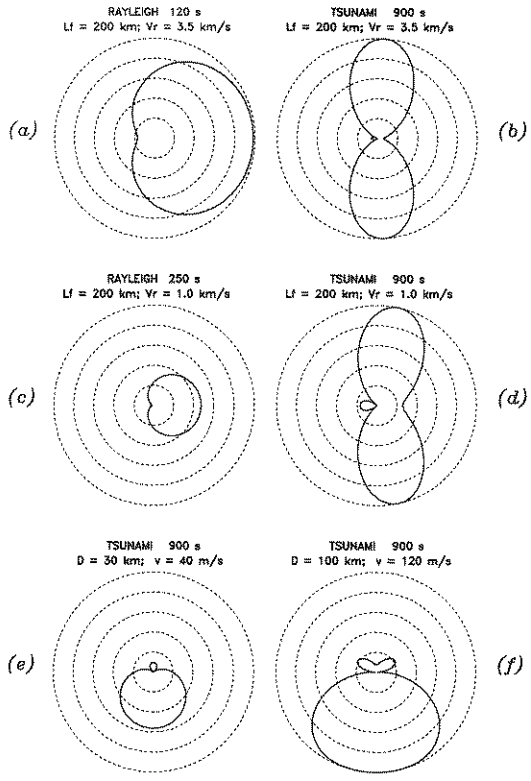

Figure 3

Theoretical directivity patterns computed for a number of tsunamigenic sources. All diagrams are azimuthal plots of the function $DIR(\phi)$ defined in (58). The dashed circles are drawn from $DIR = 0.2$ to $DIR = 1$, by steps of 0.2 units. In the top diagrams, a conventional dislocation source of length $L_f = 200$ km is rupturing to the right. (*a*): Rayleigh waves at 250 s; (*b*): Tsunami waves at 900 s. Note the narrower lobe, oriented about 90° from the rupture. In the central diagrams, we consider a slower rupture ("tsunami earthquake"); note the destructive interference of mantle Rayleigh waves (*c*), and the essentially unperturbed digram for tsunamis (*d*). In the bottom diagrams, we consider the tsunami wavefield of a landslide source, which moves towards the bottom of the figure; we consider a shallower ocean with $C = 120$ m/s. Note in (*e*) the destructive interference in all azimuths. (*f*): Only for unrealistic values of the velocity v does a constructive interference become possible; it does not, however, feature a narrow lobe comparable to those in (*b*) and (*d*).

* *If the rupture is subsonic*, i.e., $V_R < C$, then there is no solution to $\cos\phi = C/V_R$, and interference is destructive in all azimuths (Fig. 3e). Only at the longest periods, much greater than the duration of the source, can it become constructive, but then $DIR \to 1$ for all ϕ; azimuthal directivity is never present.

In this very general and classical framework, we discuss two special cases of relevance to tsunami genesis.

• We first focus on the so-called "tsunami earthquakes," generating tsunamis of disproportionate amplitude relative to their conventional seismic waves. Such events,

which include the 1946 Aleutian and 1992 Nicaraguan earthquakes (KANAMORI, 1972a; KANAMORI and KIKUCHI, 1993), have been attributed to an exceptionally slow rupture along the fault plane, due either to propagation in a sedimentary wedge (FUKAO, 1979), or to a jerky mode of rupture in the presence of asperities on the fault (TANIOKA *et al.*, 1997), with proposed velocities V_R as low as 1 km/s (POLET and KANAMORI, 2000). For such values, the rupture becomes subsonic for Rayleigh waves, with the smallest value of the parameter $C/V_R - \cos\phi$ being 2.5. For $L_f = 200$ km, the function *DIR* remains less than 0.5 in all azimuths for $T \leq 250$ s, resulting in destructive interference across the conventional seismic spectrum (Fig. 3c). However, the rupture remains hypersonic for tsunami waves ($V_R/C = 5$), which keep a very strong directivity pattern (Fig. 3d), the lobes being slightly displaced (about 10 to 15°) away from the direction perpendicular to rupture. The conclusion of this remark is that all large dislocation sources, however slow their rupture may be, generate tsunamis featuring strong directivity.

• The situation is quite different in the case of *landslides*. The evolution of an underwater landslide is obviously a more complex and less well understood process than that of a seismic dislocation, since the texture and cohesion of the material may change with time, for example during the development of a turbidity current. Nevertheless, there is ample evidence that large underwater landslides may occur over several tens of km (e.g., LEE, 1989), and possibly hundreds of seconds, occasionally thousands if a turbidity current is involved, as documented for example by the relative timing of cable breaks (HEEZEN and EWING, 1952, 1955). In this framework, and as a simplified model, Equation (58) can be used with L_f being the total displacement D of the slide, as defined in Section 2, p. 10, and V_R the velocity of the moving block, called v in (37).

In Figure 3e, we present a directivity pattern computed for $D = 30$ km and $v = 40$ m/s. These figures are taken as possibly representative of the landslide proposed for the 1946 Aleutian event. However, the value of v must be regarded as an upper bound on physically acceptable material velocities during underwater landslides. For example, in the case of the 1929 Grand Banks earthquake, PIPER *et al.* (1985, 1989) have estimated velocities of 10 to 20 m/s, both inside the valleys channeling the initial slump, and later in the turbide phase on the abyssal plain. On Frames (e) and (f), the source is moving to the bottom of the picture, to ease the comparison with the dislocation cases (earthquake rupture will propagate along the coastline, and landslides along the steepest gradient, expected to at right angles to the coast). We conclude that the parameters *DIR* remain small, expressing destructive interference in all azimuths. In (f), we investigate theoretically the unrealistic case of a sonic landslide in a shallow source region ($v = C = 120$ m/s). The interference becomes constructive in the direction of the slide, but the lobe is broad; it would take a totally unphysical value of the velocity, $v = 250$ m/s, to develop a large, narrow lobe in the far field, which, incidentally, would then be at right angles from the direction of sliding.

The conclusion of this section is that azimuthal directivity can be a robust discriminant between dislocations and landslides as generators of tsunamis in the far field. The presence of narrow lobes of strong low-frequency amplitude at transoceanic distances requires generation by a conventional dislocation.

7. Conclusion and Perspective: The 1946 Aleutian Tsunami

We have obtained theoretical results based on normal mode theory allowing the comparison of the efficiency of landslides and dislocations as generators of far-field tsunamis. We show that the modeling of tsunamis generated by landslides will be strongly affected by the quadrupolar correction derived by DAHLEN (1993), which can add a factor of 50 to 200 to the monopole force used to model the landslide. We find that landslides are always deficient generators in the far field; the bulk of their spectral amplitude is generated in a range of frequencies where significant dispersion acts to lessen the resulting amplitude of the wave. We obtain general formulae scaling the total energy carried in the far field by a tsunami wave with the size of the source; in the case of dislocations, we are able to reproduce exactly (except for a numerical factor) the expression proposed by KAJIURA (1981) using an approach based exclusively on static deformation of the ocean floor, and in particular the scaling of energy with $M_0^{4/3}$. Finally, we show that, within acceptable ranges of their kinematic parameters, landslides cannot generate strongly lobed directivity patterns in the far field. Their observation can thus be regarded as a robust discriminant of the nature of the tsunami source.

The conclusions obtained in this paper provide a framework for discussing the possible sources of the great 1946 Aleutian tsunami. We recall that this event was catastrophic both in the near field, where it eradicated the Scotch Cap lighthouse, and in the far field, where it destroyed waterfronts in Hawaii, at a cost of 159 human lives, and wrought destruction in the Marquesas Islands and possibly as far away as Antarctica. Recent field work based on the interview of elderly witnesses and on the surveying of preserved watermarks, as well as ongoing seismological investigations have quantified the following parameters:

(a) In the near field, runup reaches 42 m at Scotch Cap on Unimak Island and such values are concentrated along approximately 35 km of coastline (PLAFKER *et al.*, 2002);

(b) In the far field, runup reaches 16 m in Hawaii (LANDER and LOCKRIDGE, 1989), and between 6 and 13 m in the Marquesas and Easter Island (OKAL *et al.*, 2002), these values being measured overland, i.e., outside river beds;

(c) Runup is much lower (2.7 m) at Juan Fernández Island, suggesting a large azimuthal variation between this location and Easter (OKAL *et al.*, 2002);

(d) The seismic signature of the event is exceedingly slow, making the precise determination of its source parameters difficult. Mantle surface waves suggest a

seismic moment of at least 5×10^{28} dyn-cm (measured around 200 s), but the absence of multiple passages on Wiechert records at Uppsala rules out a further growth of this figure beyond 10^{29} dyn-cm (OKAL, 1992).

(e) The relocation of all aftershocks of the 1946 event suggests a fault length $L_f = 200$ km (OKAL and LÓPEZ, 2002).

As detailed by OKAL *et al.* (2002), the small tsunami amplitude at Juan Fernández, as compared to Easter and the Marquesas, requires a strong directivity effect focusing the energy of the tsunami in the azimuths $150 \pm 15°$, which as discussed in Section 6, is incompatible with generation by a landslide (note that our examples were computed at 900 s, the dominant period observed on far-field maregrams and reported by witnesses). Also, and as discussed in Section 3, the amplitudes of the tsunami in the far field are much too large to be explained by a landslide of an acceptable volume. Thus, the far-field characteristics of the 1946 Aleutian tsunami rule out its generation by a simple landslide. On the other hand, the extreme amplitude of runup in the near field is more than 6 times larger than any acceptable value of the slip Δu on the fault, and its distribution along the near-field coast is incompatible with generation by a dislocation (HOFFMAN *et al.*, 2002). We present as an inescapable conclusion that both phenomena – a large slow earthquake, and a major landslide – must have occurred concurrently during the 1946 Aleutian event.

Appendix 1: Corner Frequency as a Function of Moment

In this section, we derive an estimate of the scaling of the corner frequency ω_c with moment M_0, in the framework of GELLER (1976). Starting with his Equation (6), we study the evolution with frequency of the finiteness function

$$\Psi = \left| \frac{\sin \omega\chi_\tau}{\omega\chi_\tau} \cdot \frac{\sin \omega\chi_{L_f}}{\omega\chi_{L_f}} \cdot \frac{\sin \omega\chi_W}{\omega\chi_W} \right| , \tag{A1}$$

where τ is rise time, L_f source length and W source width, $\chi_\tau = \tau/2$, $\chi_{L_f} = \frac{L_f}{2V_R}$ (obtained by averaging the classical expression of directivity over azimuth), and

$$\chi_W = \frac{W}{2C} \cdot \langle |\cos\phi \sin\theta| \rangle = \frac{W}{\pi C} = \frac{L_f}{2\pi C} \tag{A2}$$

(obtained from GELLER (1976) after noticing that one averages the trigonometric function over the sphere, first over azimuth ϕ $(2/\pi)$, then over colatitude θ $(1/2)$. In these formulae, C is phase velocity, V_R rupture velocity, L_f fault length, and W fault width $(S = L_f W)$; we further assume a fault area of constant aspect ratio $W/L_f = 1/2$.

At long periods ($\omega \to 0$), $\Psi \to 1$. At short periods ($\omega \to \infty$), Ψ is at most

$$\frac{1}{\omega\chi_\tau \cdot \omega\chi_{L_f} \cdot \omega\chi_W} = \frac{8\pi V_R C}{\omega^3 \cdot \tau L_f^2} \quad . \tag{A3}$$

In scaling the source, we assume that the strain release, ε, has a constant value corresponding to the threshold at which rupture takes place in the rock, $\varepsilon_{\max}$, which we take as 10^{-4}. Then the displacement Δu along the fault plane is approximately $\varepsilon_{\max} W$, or $\Delta u = \varepsilon_{\max} \frac{L_f}{2}$, and the seismic moment

$$M_0 = \mu S \Delta u = \frac{1}{\sqrt{2}} \mu \varepsilon_{\max} S^{3/2} = \frac{1}{4} \mu L_f^3 \varepsilon_{\max} \quad , \tag{A4}$$

the constant 1/4 changing only slightly according to the geometry of rupture.

The rise time τ can be related to fault size through

$$\tau = \frac{8\sqrt{2}}{7\pi^{3/2}} \frac{L_f}{\beta} \quad , \tag{A5}$$

which follows from GELLER's (1976) Equation (5) by setting $L_f = 2W$. Hence,

$$\Psi \underset{\omega \to \infty}{\approx} 7(\pi/2)^{5/2} \frac{V_R C \beta \mu \varepsilon_{\max}}{\omega^3 M_0} = \left(\frac{\omega_c}{\omega}\right)^3 \tag{A6}$$

if we define

$$\omega_c = 7^{1/3}(\pi/2)^{5/6} \left(\frac{V_R}{\beta}\kappa\right)^{1/3} \cdot \beta \cdot \left(\frac{\mu \varepsilon_{\max}}{M_0}\right)^{1/3} \quad . \tag{A7}$$

If we further assume a constant ratio between rupture and shear velocities, $V_R/\beta = 0.8$, we obtain finally

$$\omega_c = (7/5)^{1/3} \frac{\pi^{5/6}}{2^{1/6}} \cdot \kappa^{1/3} \cdot \beta \cdot \left(\frac{\mu \varepsilon_{\max}}{M_0}\right)^{1/3} \quad . \tag{A8}$$

- In the case of Rayleigh waves in a Poisson solid, $\kappa = \sqrt{2 - 2/\sqrt{3}} = 0.9194$, and thus for a typical event in the upper mantle ($\mu = 7 \times 10^{11}$ dyn/cm^2; $\beta = 4.6$ km/s),

$$\omega_c = 4.77 \times 10^8 M_0^{-1/3} \qquad \text{or} \qquad T_c = 1.32 \times 10^{-8} M_0^{1/3} \tag{A9}$$

where ω_c is in rd/s (T_c in s), and M_0 in dyn-cm.

- In the case of a tsunami wave, $\kappa = C/\beta = \left(\frac{\rho_s g h}{\mu}\right)^{1/2}$, so that

$$\omega_c = (7/5)^{1/3} \frac{\pi^{5/6}}{2^{1/6}} \cdot \beta \cdot \left(\frac{\sqrt{\mu \rho_s g h}\, \varepsilon_{\max}}{M_0}\right)^{1/3} \tag{A10}$$

For an ocean of depth 5 km, and with the same parameters as previously used,

$$\omega_c = 1.78 \times 10^8 M_0^{-1/3} \qquad \text{or} \qquad T_c = 3.53 \times 10^{-8} M_0^{1/3} \tag{A11}$$

The corner frequency for tsunami waves is about 0.4 times that for Rayleigh waves.

Acknowledgments

I thank the conveners who invited me to the Los Angeles Workshop on landslides and tsunamis in March 2000. The comments of Bob Geller on an early version of these computations are appreciated, as well as recent discussions with Steve Kirby, Homa Lee and Bill Normark. The paper was improved through the comments of an anonymous reviewer. I am grateful to my field companions, principally Costas Synolakis and George Plafker, for helping me become acquainted first hand with the awesome scale of the 1946 Aleutian tsunami, both in the near and far fields. Parts of this work were supported by the National Science Foundation.

References

ABRAMOWITZ, M. and STEGUN I. A., *Handbook of Mathematical Functions* (Dover, New York, 1965), 1046 pp.

AIDA, I. (1977), *Simulations of Large Tsunamis Occurring in the Past off the Sanriku District*, Bull. Earthq. Res. Inst. Tokyo Univ. *52*, 71–101 (in Japanese).

AKI, K. (1966), *Generation and Propagation of G-waves from the Niigata Earthquake of June 16, 1964, Part 2. Estimation of Earthquake Moment, Released Energy, and Stress-strain Drop from the G-wave Spectrum*, Bull. Earthq. Res. Inst. Tokyo Univ. *44*, 73–88.

ALEKSEEV, A. S. and GUSYAKOV, V. K., *Numerical modeling of tsunami and seismic surface wave generation by a submarine earthquake*, Proc. Tsunami Res. Symp. (eds. R. A. Heath and M. M. Creswell) Roy. Soc. New Zealand, Wellington, (1976) pp. 243–252.

ANDO, M. (1979), *The Hawaii Earthquake of November 29, 1975: Low Dip Angle Faulting Due to Forceful Injection of Magma*, J. Geophys. Res. *84*, 7616–7626.

BEN-MENAHEM, A. (1961), *Radiation of Seismic Surface Waves from Finite Moving Sources*, Bull. Seismol. Soc. Am. *51*, 401–435.

BEN-MENAHEM, A. and ROSENMAN, M. (1972), *Amplitude Patterns of Tsunami Waves from Submarine Earthquakes*, J. Geophys. Res. *77*, 3097–3128.

DAHLEN, F. A. (1993), *Single-force Representation of Shallow Landslide Sources*, Bull. Seismol. Soc. Am. *83*, 130–143.

DZIEWONSKI, A. M. and ANDERSON, D. L. (1981), *Preliminary Reference Earth Model*, Phys. Earth Planet. Inter. *25*, 297–356.

DZIEWONSKI, A. M., EKSTRÖM, G. and MATERNOVSKAYA, N. (1999), *Centroid-moment Tensor Solutions for July–September 1998*, Phys. Earth Planet. Inter. *114*, 99–107.

EISSLER, H. K. and KANAMORI, H. (1987), *A Single-force Model for the 1975 Kalapana, Hawaii Earthquake*, J. Geophys. Res. *92*, 4827–4836.

FRYER, G. J. and WATTS, P. (2000), *The 1946 Unimak Tsunami: Near-source Modeling Confirms a Landslide*, EOS, Trans. Am. Geophys. Union *81*(48), F748–F749 (abstract).

FUKAO, Y. (1979), *Tsunami Earthquakes and Subduction Processes Near Deep-sea Trenches*, J. Geophys. Res. *84*, 2303–2314.

GELLER, R. J. (1976), *Scaling Relations for Earthquake Source Parameters and Magnitudes*, Bull. Seismol. Soc. Am. *66*, 1501–1523.

GILBERT, J. F. (1970), *Excitation of the Normal Modes of the Earth by Earthquake Sources*, Geophys. J. Roy. astr. Soc. *22*, 223–226.

GUTENBERG, B. (1939), *Tsunamis and Earthquakes*, Bull. Seismol. Soc. Am. *29*, 517–526.

HASEGAWA, H. S. and KANAMORI, H. (1987), *Source Mechanism of the Magnitude 7.2 Grand Banks Earthquake of November 18, 1929: Double-couple or Submarine Landslide?*, Bull. Seismol. Soc. Am. *77*, 1984–2004.

HEEZEN, B. C. and EWING, W. M. (1952), *Turbidity Currents and Submarine Slumps, and the 1929 Grand Banks (Newfoundland) Earthquake*, Am. J. Sci. *250*, 849–873.

HEEZEN, B. C. and EWING, W. M. (1955), *Orléansville Earthquake and Turbidity Currents*, Bull. Am. Assoc. Petrol. Geol. *39*, 505–514.

HOFFMAN, I., SYNOLAKIS, C. E. and OKAL, E. A. (2002), *Systematics of the Distribution of Tsunami Run-up along Coastlines in the Near-field for Dislocation Sources with Variable Parameters*, EOS, Trans. Am. Geophys. Union *83*(22), WP54 (abstract).

IIDA, K. (1963), *A Relation of Earthquake Energy to Tsunami Energy and the Estimation of the Vertical Displacement in a Tsunami Source*, J. Earth Sci. Nagoya Univ. *11*, 49–67.

KAJIURA, K. (1981), *Tsunami Energy in Relation to Parameters of the Earthquake Fault Model*, Bull. Earthq. Res. Inst. Tokyo Univ. *56*, 415–440.

KANAMORI, H. (1972a), *Mechanisms of Tsunami Earthquakes*, Phys. Earth Planet. Inter. *6*, 346–359.

KANAMORI, H. (1972b), *Tectonic Implications of the 1944 Tonankai and the 1946 Nankaido Earthquakes*, Phys. Earth. Planet. Inter. *5*, 129–139.

KANAMORI, H. (1985), *Non-double-couple seismic source*, Proc. XXIIIrd Gen. Assemb. Intl. Assoc Seismol. Phys. Earth Inter., Tokyo, p. 425, (abstract).

KANAMORI, H. and CIPAR, J.J. (1974), *Focal Process of the Great Chilean Earthquake, May 22, 1960*, Phys. Earth Planet. Inter. *9*, 128–136.

KANAMORI, H. and KIKUCHI, M. (1993), *The 1992 Nicaragua Earthquake; A Slow Tsunami Earthquake Associated with Subducted Sediments*, Nature *361*, 714–716.

KANAMORI, H. and STEWART, G.S. (1976), *Mode of the Strain Release along the Gibbs Fracture Zone, Mid-Atlantic Ridge*, Phys. Earth Planet. Inter. *11*, 312–332.

KANAMORI, H., GIVEN, J. W. and LAY, T. (1984), *Analysis of Seismic Body Waves Excited by the Mount St. Helens Eruption, of May 18, 1980*, J. Geophys. Res. *89*, 1856–1866.

LANDER, J. F. and LOCKRIDGE, P. A. (1989), *United States Tsunamis (including United States Possessions)*, 1690–1988, Natl. Geophys. Data Center, Natl. Atmos. Ocean. Admin. Publ. 41–2, Boulder.

LEE, H.J., *Undersea landslides; extent and significance in the Pacific Ocean.* In Proc 28th International Geological Congress Symposium on Landslides; Extent and Economic Significance (eds. E. E. Brabb and B. L. Harrod) (Balkema, Rotterdam, 1989) pp. 367–379.

LUNDGREN, P. R. and OKAL, E. A. (1988), *Slab Decoupling in the Tonga Arc: The June 22, 1977 Earthquake*, J. Geophys. Res. *93*, 13,355–13,366.

MANSINHA, L. and SMYLIE, D. E. (1971), *The Displacement Field of Inclined Faults*, Bull. Seismol. Soc. Am. *61*, 1433–1440.

MILNE, J., *Earthquakes and Other Earth Movements*, 376 pp. (Paul, Trench, Trübner & Co., London, 1898).

MONTESSUS DE BALLORE, F., *La Science Séismologique* 579 pp. (A. Colin, Paris, 1907).

OKADA, Y. (1985), *Surface Deformation Due to Shear and Tensile Faults in a Half-space*, Bull. Seismol. Soc. Am. *75*, 1135–1154.

OKAL, E. A. (1982a), *Mode-wave Equivalence and Other Asymptotic Problems in Tsunami Theory*, Phys. Earth Planet. Inter. *30*, 1–11.

OKAL, E. A. (1982b), *Higher Moment Excitation of Normal Modes and Surface Waves*, J. Phys. Earth *30*, 1–31.

OKAL, E. A. (1988), *Seismic Parameters Controlling Far-field Tsunami Amplitudes: A Review*, Natural Hazards *1*, 67–96.

OKAL, E. A. (1990), *Single Forces and Double-couples: A Theoretical Review of their Relative Efficiency for the Excitation of Seismic and Tsunami Waves*, J. Phys. Earth *38*, 445–474.

OKAL, E. A. (1991), *Erratum (to "Seismic Parameters Controlling Far-field Tsunami Amplitudes: A Review")*, Natural Hazards *4*, 433.

OKAL, E. A. (1992), *Use of the Mantle Magnitude M_m for the Reassessment of the Seismic Moment of Historical Earthquakes. I: Shallow Events*, Pure Appl. Geophys. *139*, 17–57.

OKAL, E A. and LÓPEZ, A.M. (2002), *New Seismological Results on the 1946 Aleutian Earthquake*, EOS, Trans. Am. Geophys. Union *83*(22), WP54, (abstract).

OKAL, E. A. and SYNOLAKIS, C. E. (2003), *Theoretical Comparison of Tsunamis from Dislocations and Landslides*, Pure Appl. Geophys. *160*, 2177–2188.

OKAL, E. A. and TALANDIER, J. (1989), *M_m: A Variable Period Mantle Magnitude*, J. Geophys. Res. *94*, 4169–4193.

OKAL, E. A. and TALANDIER, J. (1991), *Single-station Estimates of the Seismic Moment of the 1960 Chilean and 1964 Alaskan Earthquakes, Using the Mantle Magnitude M_m*, Pure Appl. Geophys. *136*, 103–126.

OKAL, E. A., SYNOLAKIS, C. E., FRYER, G .J., HEINRICH, P., BORRERO, J. C., RUSCHER, C., ARCAS, D., GUILLE, G. and ROUSSEAU, D. (2002), *A Field Survey of the 1946 Aleutian Tsunami in the Far Field*, Seismol. Res. Letts. *73*, 490–503.

PIPER, D. J. W., SHOR, A. N., FARRE, J. A., O'CONNELL, S. and JACOBI, R. (1985), *Sediment Slides and Turbidity Currents on the Laurentian Fan: Sidescan Sonar Investigations near the Epicenter of the 1929 Grand Banks Earthquake*, Geology *13*, 538–541.

PIPER, D. J. W., SHOR, A. N. and HUGHES CLARKE, J. E. (1988), *The 1929 "Grand Banks" Earthquake, Slump and Turbidity Current*, Geol. Soc. Am. Sp. Paper *229*, 77–92.

PLAFKER, G., OKAL, E. A. and SYNOLAKIS, C. E. (2002), *A New Survey of the 1946 Aleutian Tsunami in the Near Field: Evidence for a Large Underwater Landslide at Davidson Bank*, Seismol. Soc. Am. *73*, 259 (abstract).

POD"YAPOL'SKII, G. S., *Generation of the Tsunami Wave by the Earthquake*. In *Tsunamis in the Pacific Ocean* (ed. W. M. Adams) (East-West Center Press, Honolulu, 1970) pp. 19–32.

POLET, Y. and KANAMORI, H. (2000), *Shallow Subduction Zone Earthquakes and their Tsunamigenic Potential*, Geophys. J. Intl. *142*, 684–702.

SAITO, M. (1967), *Excitation of Free Oscillations and Surface Waves by a Point Source in a Vertically Heterogeneous Earth*, J. Geophys. Res. *72*, 3689–3699.

SWEET, S. and SILVER, E. A. (2003), *Tectonics and Slumping in the Source Region of the 1998 Papua New Guinea Tsunami from Seismic Reflection Images*, Pure Appl. Geophys. *160*, 1945–1968.

SYNOLAKIS, C. E., BARDET, J. -P., BORRERO, J.C., DAVIES, H.L., OKAL, E.A., SILVER, E.A., SWEET, S. and TAPPIN, D.R. (2002), *The Slump Origin of the 1998 Papua New Guinea Tsunami*, Proc. Roy. Soc. (London), Ser. A *458*, 763–789.

TALANDIER, J. and OKAL, E. A. (1979), *Human Perception of T Waves: The June 22, 1977 Tonga Earthquake Felt on Tahiti*, Bull. Seismol. Soc. Am. *69*, 1475–1486.

TANIOKA, Y., RUFF, L. J. and SATAKE, K. (1997), *What Controls the Lateral Variation of Large Earthquake Occurrence along the Japan Trench?*, The Island Arc *6*, 261–266.

VVEDENSKAYA (1956), *Opredelenie polej smeshchenij pri zemletryasenniyakh s pomoshch'yu teorii dislokatsij*, Izv. Akad. Nauk SSSR, Ser. Geofiz. *6*, 277–284 (in Russian).

WARD, S. N. (1980), *Relationship of Tsunami Generation and an Earthquake Source*, J. Phys. Earth *28*, 441–474.

WARD, S. N. (1981), *On Tsunami Nucleation: I. A Point Source*, J. Geophys. Res. *86*, 7895–7900.

WARD, S. N. (1982), *On Tsunami Nucleation: II. An Instantaneous Modulated Line Source*, Phys. Earth Planet. Inter. *27*, 273–285.